American Journal of Computational Mathematics, 2014, 4, 289-303
Published Online September 2014 in SciRes. http://www.scirp.org/journal/ajcm
http://dx.doi.org/10.4236/ajcm.2014.44025

Scientific Research

Deterministic Chaos of *N* Stochastic Waves in Two Dimensions

Victor A. Miroshnikov

Department of Mathematics, College of Mount Saint Vincent, New York, USA
Email: victor.miroshnikov@mountsaintvincent.edu

Received 20 June 2014; revised 23 July 2014; accepted 2 August 2014

Abstract

Kinematic exponential Fourier (KEF) structures, dynamic exponential (DEF) Fourier structures, and KEF-DEF structures with time-dependent structural coefficients are developed to examine kinematic and dynamic problems for a deterministic chaos of *N* stochastic waves in the two-dimensional theory of the Newtonian flows with harmonic velocity. The Dirichlet problems are formulated for kinematic and dynamics systems of the vorticity, continuity, Helmholtz, Lamb-Helmholtz, and Bernoulli equations in the upper and lower domains for stochastic waves vanishing at infinity. Development of the novel method of solving partial differential equations through decomposition in invariant structures is resumed by using experimental and theoretical computation in Maple™. This computational method generalizes the analytical methods of separation of variables and undetermined coefficients. Exact solutions for the deterministic chaos of upper and lower cumulative flows are revealed by experimental computing, proved by theoretical computing, and justified by the system of Navier-Stokes PDEs. Various scenarios of a developed wave chaos are modeled by 3*N* parameters and 2*N* boundary functions, which exhibit stochastic behavior.

Keywords

Stochastic Waves, Invariant Structures, Experimental Computation, Theoretical Computation

1. Introduction

The two-dimensional (2d) Navier-Stokes system of partial differential equations (PDEs) for a Newtonian fluid with a constant density ρ and a constant kinematic viscosity ν in a gravity field g is

$$\frac{\partial \boldsymbol{v}}{\partial t}+(\boldsymbol{v}\cdot\nabla)\boldsymbol{v}=-\frac{1}{\rho}\nabla p_t+\nu\Delta\boldsymbol{v}+\boldsymbol{g}, \tag{1}$$

How to cite this paper: Miroshnikov, V.A. (2014) Deterministic Chaos of *N* Stochastic Waves in Two Dimensions. *American Journal of Computational Mathematics*, **4**, 289-303. http://dx.doi.org/10.4236/ajcm.2014.44025

$$\nabla \cdot \boldsymbol{v} = 0, \tag{2}$$

where $\boldsymbol{v} = (u, 0, w)$ is a vector field of the flow velocity, $\boldsymbol{g} = (0, 0, -g_z)$ is a vector field of the gravitational acceleration, p_t is a scalar field of the total pressure, $\nabla = (\partial/\partial x, 0, \partial/\partial z)$ and $\Delta = \partial^2/\partial x^2 + \partial^2/\partial z^2$ are the gradient and the Laplacian in the 2d Cartesian coordinate system $\boldsymbol{x} = (x, 0, z)$ of the three-dimensional (3d) space with unit vectors $(\boldsymbol{i}, \boldsymbol{j}, \boldsymbol{k})$, respectively, and t is time.

By a flow vorticity $\boldsymbol{\omega} = (0, \upsilon, 0)$ of the velocity field

$$\nabla \times \boldsymbol{v} = \boldsymbol{\omega}, \tag{3}$$

Equation (1) may be written into the Lamb-Pozrikidis form [1] [2]

$$\frac{\partial \boldsymbol{v}}{\partial t} + \nabla\left(\frac{1}{2}\boldsymbol{v} \cdot \boldsymbol{v} + \frac{p_t}{\rho} - \boldsymbol{g} \cdot \boldsymbol{x}\right) + \boldsymbol{\omega} \times \boldsymbol{v} + \nu \nabla \times \boldsymbol{\omega} = 0, \tag{4}$$

which sets a dynamic balance of inertial, potential, vortical, and viscous forces, respectively.

Using a dynamic pressure per unit mass [3]

$$p_d = \frac{p_t - p_0}{\rho} - \boldsymbol{g} \cdot \boldsymbol{x}, \tag{5}$$

where p_0 is a reference pressure, a kinetic energy per unit mass $k_e = \boldsymbol{v} \cdot \boldsymbol{v}/2$, the 2d Helmholtz decomposition [4] of the velocity field

$$\boldsymbol{v} = \nabla \phi + \nabla \times \boldsymbol{\psi}, \tag{6}$$

and the vortex force

$$\boldsymbol{\omega} \times \boldsymbol{v} = \nabla d + \nabla \times \boldsymbol{a}, \tag{7}$$

Equation (4) is reduced to the Lamb-Helmholtz PDE [5]

$$\nabla b_e + \nabla \times \boldsymbol{h}_e = 0 \tag{8}$$

for a scalar Bernoulli potential and a vector Helmholtz potential, respectively,

$$b_e = \frac{\partial \phi}{\partial t} + p_d + k_e + d, \tag{9}$$

$$\boldsymbol{h}_e = \frac{\partial \boldsymbol{\psi}}{\partial t} + \nu \boldsymbol{\omega} + \boldsymbol{a}, \tag{10}$$

where ϕ and d are scalar potentials, $\boldsymbol{\psi} = (0, \eta, 0)$ and $\boldsymbol{a} = (0, b, 0)$ are vector potentials, η and b are pseudovector potentials of $\boldsymbol{v}$ and $\boldsymbol{\omega} \times \boldsymbol{v}$, respectively. The Lamb-Helmholtz PDE (8) means a dynamic balance between potential and vortical forces of the Navier-Stokes PDE (1), which are separated completely. Reduction of (1) to (8) means the potential-vortical duality of the Navier-Stokes PDE since writing equation (8) as

$$\boldsymbol{n}_s = -\nabla b_e = \nabla \times \boldsymbol{h}_e \tag{11}$$

shows that a virtual force $\boldsymbol{n}_s$ of (1) may be represented both in the potential form $\boldsymbol{n}_s = -\nabla b_e$ and the vortical form $\boldsymbol{n}_s = \nabla \times \boldsymbol{h}_e$.

The exponential Fourier eigenfunctions obtained by the classical method of separation of variables of the 2d Laplace equation in [1] and [4] were primarily used for a linear part of the kinematic problem for free-surface waves of the theory of the ideal fluid with $\nu = 0$ in [6]. This analytical method was recently developed into the computational method of solving PDEs by decomposition into invariant structures. Topological flows away from boundaries were computed by the Boussinesq-Rayleigh-Taylor structures in [3]. Spatiotemporal cascades of exposed and hidden perturbations of the Couette flow were modeled by the trigonometric Taylor structures and the trigonometric-hyperbolic structures, respectively, in [7]. Dual perturbations of the Poiseuille-Hagen flow were treated by the invariant trigonometric, hyperbolic, and elliptic structures in [8]. Exact solutions for the conservative interaction of N internal waves were recently obtained by experimental and theoretical computing with kinematic Fourier (KF) structures with space-dependent structural coefficients and exponential kinematic Fourier (KEF) structures, dynamic exponential Fourier (DEF) structures, and KEF-DEF structures with constant structural coefficients in [5].

To examine linear and nonlinear parts of kinematic and dynamic problems for 2d stochastic waves in the theory of Newtonian flows with harmonic velocity, the KEF structures, the DEF structures, and the KEF-DEF structures with time-dependent structural coefficients are developed in the current paper. The structure of this paper is as follows. The KEF structures are used to compute theoretical solutions of the kinematic problems for the velocity components and the dual potentials of the velocity field in Section 2. The KEF and KEF-DEF structures are employed for theoretical computation of the dynamic problems for the Helmholtz and Bernoulli potentials, the kinetic energy, and the total pressure in Section 3. Verification of the experimental and theoretical solutions is also provided in Section 3. Various scenarios of a developed wave chaos are treated in Section 4. A summary of main results is given in Section 5.

2. Kinematic Problems for Internal Waves

The following solutions and admissible boundary conditions for the kinematic problems of Section 2 in the KEF and DEF structures with time-dependent coefficients were primarily computed via experimental programming techniques, which use lists of equations and expressions of Maple™ in the virtual environment of a global variable *Eqs* with 25 procedures of 600 code lines in total.

2.1. Formulation of Theoretical Kinematic Problems for the Velocity Field

Theoretical kinematic problems for harmonic velocity components $u = u(x,z,t)$ and $w = w(x,z,t)$ of a cumulative flow $\boldsymbol{v} = u\boldsymbol{i} + w\boldsymbol{k}$ of a Newtonian fluid are given by vanishing the *y*-component of the vorticity Equation (3) and the continuity Equation (2), respectively,

$$\frac{\partial u}{\partial z} - \frac{\partial w}{\partial x} = 0, \quad \frac{\partial u}{\partial x} + \frac{\partial w}{\partial z} = 0. \tag{12}$$

To consider a deterministic chaos of *N* internal, stochastic waves, the cumulative flow is decomposed into a superposition of local flows

$$u = \sum_{n=1}^{N} u_n(x,z,t), \quad w = \sum_{n=1}^{N} w_n(x,z,t), \tag{13}$$

such that the local vorticity and continuity equations are

$$\frac{\partial u_n}{\partial z} - \frac{\partial w_n}{\partial x} = 0, \quad \frac{\partial u_n}{\partial x} + \frac{\partial w_n}{\partial z} = 0. \tag{14}$$

where $n = 1, 2, \cdots, N$.

An upper cumulative flow is specified by the Dirichlet condition in the KF structure on a lower boundary $z = 0$ of an upper domain $x \in (-\infty, \infty)$ and $z \in [0, \infty)$ (see **Figure 1**).

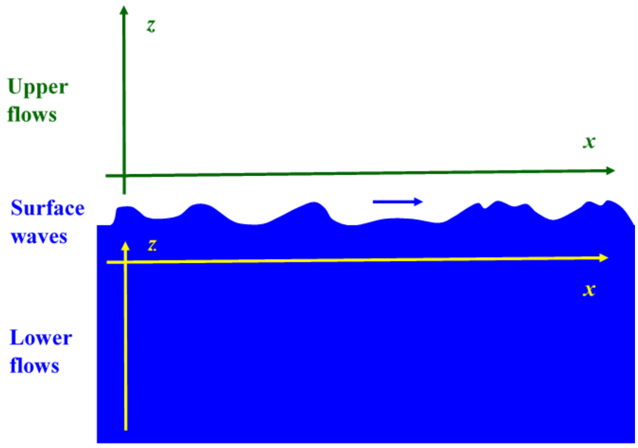

Figure 1. Configuration of upper and lower domains for stochastic waves.

$$w\big|_{z=0} = \sum_{n=1}^{N} \left[Fw_n(t) ca_n + Gw_n(t) sa_n \right], \tag{15}$$

and a vanishing condition as $z \to \infty$

$$w\big|_{z=\infty} = 0. \tag{16}$$

A lower cumulative flow is identified by the Dirichlet condition on an upper boundary $z = 0$ of a lower domain $x \in (-\infty, \infty)$ and $z \in (-\infty, 0]$ (see **Figure 1**).

$$w\big|_{z=0} = \sum_{n=1}^{N} \left[Fw_n(t) ca_n + Gw_n(t) sa_n \right], \tag{17}$$

and a vanishing condition as $z \to \infty$

$$w\big|_{z=-\infty} = 0. \tag{18}$$

Thus, an effect of surface waves on the internal waves is described by the Dirichlet conditions (15) and (17). Here, a structural notation

$$ca_n = \cos(\alpha_n), \quad sa_n = \sin(\alpha_n), \tag{19}$$

is used for kinematic structural functions ca_n and sa_n, where $Fw_n(t)$ and $Gw_n(t)$ are time-dependent boundary functions, $\alpha_n = \rho_n X_n$ is an argument of the kinematic and dynamic structural functions, $X_n = x - Cx_n t - Xa_n$ is a propagation variable, ρ_n is a wave number, Cx_n is a celerity, and Xa_n is an initial coordinate for all n. Similar to [5], boundary conditions for u_n are then redundant since boundary parameters of u_n depend on boundary parameters of w_n for the upper and lower flows, respectively, as

$$u\big|_{z=0} = -\sum_{n=1}^{N} \left[Gw_n(t) ca_n - Fw_n(t) sa_n \right], \tag{20}$$

$$u\big|_{z=0} = \sum_{n=1}^{N} \left[Gw_n(t) ca_n - Fw_n(t) sa_n \right]. \tag{21}$$

Similarly to w, u vanishes as $z \to \pm\infty$

$$u\big|_{z=\infty} = 0, \quad u\big|_{z=-\infty} = 0, \tag{22}$$

for the upper and lower cumulative flows, respectively.

2.2. Theoretical Solutions for the Velocity Field

Theoretical solutions of kinematic problems (12)-(18) are constructed in the KEF structure $p(x,z,t)$ of two spatial variables x, u and time t with a general term p_n, which in the structural notation may be written as

$$p(x,z,t) = \sum_{n=1}^{N} p_n(x,z,t) = \sum_{n=1}^{N} \left[fp_n(t) ca_n + gp_n(t) sa_n \right] \exp(\mp \rho_n z), \tag{23}$$

where signs "–" and "+" of the exponential term refer to the upper and lower flows, respectively, first letters f and g of structural coefficients $fp_n(t)$ and $gp_n(t)$ refer to the kinematic structural functions ca_n, sa_n and a second letter to the expanded variable p. General terms of the velocity components of the upper and lower flows become, respectively,

$$u_n = \left[fu_n(t) ca_n + gu_n(t) sa_n \right] \exp(\mp \rho_n z), \tag{24}$$

$$w_n = \left[fw_n(t) ca_n + gw_n(t) sa_n \right] \exp(\mp \rho_n z). \tag{25}$$

It may be shown that spatial derivatives of p_n are

$$\frac{\partial p_n}{\partial x} = \rho_n \left[gp_n(t) ca_n - fp_n(t) sa_n \right] \exp(\mp \rho_n z), \tag{26}$$

$$\frac{\partial p_n}{\partial z} = \mp\rho_n\left[fp_n(t)ca_n + gp_n(t)sa_n\right]\exp(\mp\rho_n z). \tag{27}$$

Application of (26) (27) to (24) (25), substitution in (14), collection of the structural functions, and vanishing their coefficients reduce two vorticity and continuity PDEs to the following system of four vorticity and continuity algebraic equations (AEs) with respect to $fu_n(t),\ gw_n(t),\ fw_n(t),\ gu_n(t)$ for the upper flows

$$-fu_n(t) - gw_n(t) = 0,\ \ fw_n(t) - gu_n(t) = 0, \tag{28}$$

$$-fu_n(t) - gw_n(t) = 0,\ \ -fw_n(t) + gu_n(t) = 0, \tag{29}$$

the lower flows

$$fu_n(t) - gw_n(t) = 0,\ \ fw_n(t) + gu_n(t) = 0, \tag{30}$$

$$-fu_n(t) + gw_n(t) = 0,\ \ fw_n(t) + gu_n(t) = 0, \tag{31}$$

and all $x, z, t, Xa_n, Cx_n, \rho_n, ca_n sa_n, fu_n(t), gu_n(t), fw_n(t), gw_n(t)$.

Solving AEs (28) and (30) yields for the upper and lower flows, respectively,

$$fu_n(t) = -gw_n(t),\ \ gu_n(t) = fw_n(t), \tag{32}$$

$$fu_n(t) = gw_n(t),\ \ gu_n(t) = -fw_n(t). \tag{33}$$

Substitution of solutions (32) in (29) and (33) in (31) reduces them to identities, showing that vorticity and continuity AEs (28)-(31) are compatible. Finally, substitution of (32) (33) in the KEF structures (24) (25) and solving the Dirichlet boundary conditions (15) and (17) with respect to $fw_n(t)$ and $gw_n(t)$ produces velocity components for the upper and lower cumulative flow, respectively,

$$\begin{aligned} u(x,z,t) &= \mp\sum_{n=1}^{N}\left[Gw_n(t)ca_n - Fw_n(t)sa_n\right]\exp(\mp\rho_n z), \\ w(x,z,t) &= \sum_{n=1}^{N}\left[Fw_n(t)ca_n + Gw_n(t)sa_n\right]\exp(\mp\rho_n z), \end{aligned} \tag{34}$$

while vanishing boundary conditions (16) and (18) are obviously satisfied.

2.3. The DEF Structure and Theoretical Jacobian Determinants of the Velocity Field

Define two KEF structures $l(x,z,t)$ and $h(x,z,t)$ with general terms l_n and h_m by using the generalized Einstein notation for summation that is extended for exponents in [5]

$$\begin{aligned} l &= \sum_{n=1}^{N} l_n = \left[fl_n(t)ca_n + gl_n(t)sa_n\right]\exp(\mp\rho_n z), \\ h &= \sum_{m=1}^{N} h_m = \left[fh_m(t)ca_m + gh_m(t)sa_m\right]\exp(\mp\rho_n z). \end{aligned} \tag{35}$$

Following [5], define structural functions $Cad_{n,m}, Cas_{n,m}, Sad_{n,m}$, and $Sas_{n,m}$ of the DEF structure

$$\begin{aligned} Cad_{n,m} &= \cos(\alpha_n - \alpha_m),\ \ Cas_{n,m} = \cos(\alpha_n + \alpha_m), \\ Sad_{n,m} &= \sin(\alpha_n - \alpha_m),\ \ Sas_{n,m} = \sin(\alpha_n + \alpha_m), \end{aligned} \tag{36}$$

where capital letters C and S stand for dynamic structural functions cosine and sine, letter a for arguments α_n, α_m, letters s and d for sum and difference of arguments α_n and α_m.

Computation of a general term $p_{n,n} = l_n h_n$ by summation of diagonal terms yields

$$\begin{aligned} p_{n,n} = \{ & fl_n(t)fh_n(t) + gl_n(t)gh_n(t) + \left[fl_n(t)fh_n(t) - gl_n(t)gh_n(t)\right]Cas_{n,n} \\ & + \left[fl_n(t)gh_n(t) + fh_n(t)gl_n(t)\right]Sas_{n,n}\}\exp(\mp 2\rho_n z)/2. \end{aligned} \tag{37}$$

A general term $p_{n,m} = l_n h_m$ computed by rectangular summation of non-diagonal terms becomes

$$p_{n,m}=\{[fl_n(t)fh_m(t)+gl_n(t)gh_m(t)]Cad_{n,m}+[fl_n(t)fh_m(t)-gl_n(t)gh_m(t)]Cas_{n,m}$$
$$+[-fl_n(t)gh_m(t)+fh_m(t)gl_n(t)]Sad_{n,m}+[fl_n(t)gh_m(t)+fh_m(t)gl_n(t)]Sas_{n,m}\}$$
$$\times\exp[\mp(\rho_n+\rho_m)z]/2. \quad (38)$$

By triangular summation, $p_{n,m}$ is reduced to

$$p_{n,m}=\{[fl_n(t)fh_m(t)+fl_m(t)fh_n(t)+gl_n(t)gh_m(t)+gl_m(t)gh_n(t)]Cad_{n,m}$$
$$+[fl_n(t)fh_m(t)+fl_m(t)fh_n(t)-gl_n(t)gh_m(t)-gl_m(t)gh_n(t)]Cas_{n,m}$$
$$+[-fl_n(t)gh_m(t)+fl_m(t)gh_n(t)-fh_n(t)gl_m(t)+fh_m(t)gl_n(t)]Sad_{n,m}$$
$$+[fl_n(t)gh_m(t)+fl_m(t)(t)gh_n(t)+fh_n(t)gl_m(t)+fh_m(t)gl_n(t)]Sas_{n,m}\}\exp[\mp(\rho_n+\rho_m)z]/2. \quad (39)$$

By (37) and (39), summation formula for the product of the KEF structures may be written as the DEF structure with time-dependent structural coefficients

$$p(x,z,t)=l(x,z,t)h(x,z,t)=\frac{1}{2}\sum_{n=1}^{N}[fdp_{n,n}(t)+fsp_{n,n}(t)Cas_{n,n}+gsp_{n,n}(t)Sas_{n,n}]\exp(\mp2\rho_n z)$$
$$+\frac{1}{2}\sum_{n=1}^{N-1}\sum_{m=n+1}^{N}[fdp_{n,m}(t)Cad_{n,m}+fsp_{n,m}(t)Cas_{n,m}+gdp_{n,m}(t)Sad_{n,m}$$
$$+gsp_{n,m}(t)Sas_{n,m}\exp[\mp(\rho_n+\rho_m)z] \quad (40)$$

with the following structural coefficients:

$$fdp_{n,n}(t)=fl_n(t)fh_n(t)+gl_n(t)gh_n(t),$$
$$fsp_{n,n}(t)=fl_n(t)fh_n(t)-gl_n(t)gh_n(t),$$
$$gsp_{n,n}(t)=fl_n(t)gh_n(t)+fh_n(t)gl_n(t),$$
$$fdp_{n,m}(t)=fl_n(t)fh_m(t)+fl_m(t)fh_n(t)+gl_n(t)gh_m(t)+gl_m(t)gh_n(t), \quad (41)$$
$$fsp_{n,m}(t)=fl_n(t)fh_m(t)+fl_m(t)fh_n(t)-gl_n(t)gh_m(t)-gl_m(t)gh_n(t),$$
$$gdp_{n,m}(t)=-fl_n(t)gh_m(t)+fl_m(t)gh_n(t)-fh_n(t)gl_m(t)+fh_m(t)gl_n(t),$$
$$gsp_{n,m}(t)=fl_n(t)gh_m(t)+fl_m(t)gh_n(t)+fh_n(t)gl_m(t)+fh_m(t)gl_n(t),$$

where first two letters fd, fs, gd, and gs of structural coefficients $fdp_{n,m}, fsp_{n,m}, gdp_{n,m}$, and $gsp_{n,m}$ stand for dynamic structural functions Cad_n, Cas_n, Sad_n, and Sas_n, respectively, and a third letter for variable *p*.

Computation of local JDs for the velocity components of the upper and lower flow, respectively, yields

$$\frac{\partial u_n}{\partial x}\frac{\partial w_n}{\partial z}-\frac{\partial u_n}{\partial z}\frac{\partial w_n}{\partial x}=-[Fw_n^2(t)+Gw_n^2(t)]\rho_n^2\exp(\mp2\rho_n z). \quad (42)$$

Thus, velocity components u_n and w_n are independent for non-trivial structural coefficients $Fw_n(t)$ and $Gw_n(t)$ since the local JDs vanish when $Fw_n^2(t)+Gw_n^2(t)=0$.

Computation of a global JD by using (40) (41) for velocity components of the upper and lower cumulative flows (34) with slant internal waves gives

$$J_g=\frac{\partial u}{\partial x}\frac{\partial w}{\partial z}-\frac{\partial u}{\partial z}\frac{\partial w}{\partial x}=-\sum_{n=1}^{N}[Fw_n^2(t)+Gw_n^2(t)]\rho_n^2\exp(\mp2\rho_n z)$$
$$-2\sum_{n=1}^{N-1}\sum_{m=n+1}^{N}\{[Fw_n(t)Fw_m(t)+Gw_n(t)Gw_m(t)]Cad_{n,m}$$
$$+[-Fw_n(t)Gw_m(t)+Fw_m(t)Gw_n(t)]Sad_{n,m}\}\rho_n\rho_m\exp[\mp(\rho_n+\rho_m)z]. \quad (43)$$

So, J_g is a superposition of a propagation JD with general term $Jc_{n,n}$ proportional to $Cad_{n,n}\equiv1$, an interaction JD with $Jc_{n,m}$ proportional to $Cad_{n,m}$, and an interaction JD with $Js_{n,m}$ proportional to $Sad_{n,m}$, which describe interaction between parallel and orthogonal internal waves, respectively.

$Jc_{n,n}$ coincides with local JDs (42). They describe propagation of internal waves and vanish only for vanishing waves with $Fw_n^2(t)+Gw_n^2(t)=0$. $Js_{n,m}$ vanishes for parallel waves with

$$\frac{Fw_m(t)}{Fw_n(t)}=\frac{Gw_m(t)}{Gw_n(t)}=A_{n,m}(t). \tag{44}$$

Global JD (43) then becomes

$$\begin{aligned} J_p &= -\sum_{n=1}^{N}\left[Fw_n^2(t)+Gw_n^2(t)\right]\rho_n^2\exp(\mp 2\rho_n z) \\ &\quad -2\sum_{n=1}^{N-1}\sum_{m=n+1}^{N}A_{n,m}(t)\left[Fw_n^2(t)+Gw_n^2(t)\right]Cad_{n,m}\rho_n\rho_m\exp\left[\mp(\rho_n+\rho_m)z\right]. \end{aligned} \tag{45}$$

Thus, the global JD does not vanish for parallel waves with non-vanishing $Fw_n^2(t)+Gw_n^2(t)$.

$Jc_{n,m}$ vanishes for orthogonal waves with

$$\frac{Fw_m(t)}{Gw_n(t)}=-\frac{Gw_m(t)}{Fw_n(t)}=B_{n,m}(t). \tag{46}$$

In this case, global JD (43) is reduced to

$$\begin{aligned} J_o &= -\sum_{n=1}^{N}\left[Fw_n^2(t)+Gw_n^2(t)\right]\rho_n^2\exp(\mp 2\rho_n z) \\ &\quad -2\sum_{n=1}^{N-1}\sum_{m=n+1}^{N}B_{n,m}(t)\left[Fw_n^2(t)+Gw_n^2(t)\right]Sad_{n,m}\rho_n\rho_m\exp\left[\mp(\rho_n+\rho_m)z\right]. \end{aligned} \tag{47}$$

So, the global JD does not vanish also for orthogonal waves with non-vanishing $Fw_n^2(t)+Gw_n^2(t)$. In the general case of slant internal waves (43), both $Js_{n,m}$ and $Jc_{n,m}$ are non-vanishing. Therefore, both propagating and interacting waves are independent for structural coefficients with $Fw_n^2(t)+Gw_n^2(t)\neq 0$ for all *n*.

2.4. Theoretical Solutions for the Kinematic Potentials in the KEF Structures

Theoretical kinematic problems for cumulative pseudovector potential $\eta(x,z,t)$ and cumulative scalar potential $\phi(x,z,t)$ of $\boldsymbol{v}$ are set by the global Helmholtz PDEs (6)

$$\frac{\partial\eta}{\partial z}+u=0,\quad \frac{\partial\eta}{\partial x}-w=0, \tag{48}$$

$$\frac{\partial\phi}{\partial x}-u=0,\quad \frac{\partial\phi}{\partial z}-w=0, \tag{49}$$

since the potential-vortical duality the velocity field admits two presentations: $\boldsymbol{v}=\nabla\phi$ for $\boldsymbol{\psi}=0$ and $\boldsymbol{v}=\nabla\times\boldsymbol{\psi}$ for $\phi=0$. The cumulative kinematic potentials are decomposed into a superposition of local kinematic potentials

$$\eta=\sum_{n=1}^{N}\eta_n(x,z,t),\quad \phi=\sum_{n=1}^{N}\phi_n(x,z,t), \tag{50}$$

such that the local Helmholtz PDEs are

$$\frac{\partial\eta_n}{\partial z}+u_n=0,\quad \frac{\partial\eta_n}{\partial x}-w_n=0, \tag{51}$$

$$\frac{\partial\phi_n}{\partial x}-u_n=0,\quad \frac{\partial\phi_n}{\partial z}-w_n=0, \tag{52}$$

where $n=1,2,\cdots,N$.

Construct general terms of the kinematic potentials of the local flows in the KEF structure with time-dependent coefficients

$$\eta_n = \left[fe_n(t) ca_n + ge_n(t) sa_n \right] \exp(\mp \rho_n z), \tag{53}$$

$$\varphi_n = \left[fp_n(t) ca_n + gp_n(t) sa_n \right] \exp(\mp \rho_n z). \tag{54}$$

Application of (26) (27) to (53) (54), substitution in the Helmholtz PDEs (51) (52), collection of the structural functions, and vanishing their coefficients reduce four Helmholtz PDEs to the following system of eight Helmholtz AEs for the upper flows

$$\begin{aligned} -\rho_n fe_n(t) - Gw_n(t) = 0, \ \ \rho_n ge_n(t) - Fw_n(t) = 0, \\ -\rho_n fp_n(t) - Fw_n(t) = 0, \ \ \rho_n gp_n(t) + Gw_n(t) = 0, \end{aligned} \tag{55}$$

$$\begin{aligned} -\rho_n fe_n(t) - Gw_n(t) = 0, \ \ -\rho_n ge_n(t) + Fw_n(t) = 0, \\ -\rho_n fp_n(t) - Fw_n(t) = 0, \ \ -\rho_n gp_n(t) - Gw_n(t) = 0, \end{aligned} \tag{56}$$

the lower flows

$$\begin{aligned} -\rho_n fe_n(t) - Gw_n(t) = 0, \ \ \rho_n ge_n(t) - Fw_n(t)(t) = 0, \\ -\rho_n fp_n(t) + Fw_n(t) = 0, \ \ \rho_n gp_n(t) - Gw_n(t) = 0, \end{aligned} \tag{57}$$

$$\begin{aligned} \rho_n fe_n(t) + Gw_n(t) = 0, \ \ \rho_n ge_n(t) - Fw_n(t) = 0, \\ \rho_n fp_n(t) - Fw_n(t) = 0, \ \ \rho_n gp_n(t) - Gw_n(t) = 0, \end{aligned} \tag{58}$$

and all $x, z, t, Xa_n, Cx_n, \rho_n, ca_n, sa_n, fe_n(t), ge_n(t), fp_n(t), gp_n(t), Fw_n(t)$, and $Gw_n(t)$.

Solving AEs (55) and (57) with respect to time-dependent structural coefficients $fe_n(t), ge_n(t), fp_n(t)$, and $gp_n(t)$ gives for the upper and lower flows, respectively,

$$\begin{aligned} fe_n(t) = -\frac{Gw_n(t)}{\rho_n}, \ \ ge_n(t) = \frac{Fw_n(t)}{\rho_n}, \\ fp_n(t) = \mp\frac{Fw_n(t)}{\rho_n}, \ \ gp_n(t) = \mp\frac{Gw_n(t)}{\rho_n}. \end{aligned} \tag{59}$$

Substitution of solutions (59) in AEs (56) and (58) reduces them to identities. Finally, substitution of structural coefficients (59) in the KEF structures (53) (54) and superpositions (50) yields the cumulative kinematic potentials in the KEF structures for the upper and lower cumulative flows, respectively,

$$\begin{aligned} \eta(x,z,t) = -\sum_{n=1}^{N} \frac{Gw_n(t) ca_n - Fw_n(t) sa_n}{\rho_n} \exp(\mp \rho_n z), \\ \phi(x,z,t) = \mp\sum_{n=1}^{N} \frac{Fw_n(t) ca_n + Gw_n(t) sa_n}{\rho_n} \exp(\mp \rho_n z). \end{aligned} \tag{60}$$

The theoretical solutions in the KEF and DEF structures for the kinematic problems of Section 2 were computed utilizing theoretical programming methods with symbolic general terms in the virtual environment of a global variable *Eqt* with 21 procedures of 522 Maple code lines in total. The theoretical formulas for velocity components (34), the products of the KEF structures (40) (41), and the kinematic potentials (60) of the upper and lower cumulative flows were justified by the correspondent experimental solutions for $N = 1, 3, 10$.

3. Dynamic Problems for Internal Waves

The following solutions for the dynamic problems of Section 3 in the KEF, DEF, and KEF-DEF structures were primarily computed by experimental programming with lists of equations and expressions in the virtual environment of the global variable *Eqs* with 18 procedures of 470 code lines in total.

3.1. Theoretical Solutions for the Dynamic Potentials in the KEF Structures

Theoretical dynamic problems in the KF structures for the Helmholtz and Bernoulli potentials of the cumulative flows are set by the Lamb-Helmholtz PDEs (8)-(10) in the vortical presentation with $\phi = 0$

$$\frac{\partial b_e}{\partial x} - \frac{\partial h_e}{\partial z} = 0, \quad \frac{\partial b_e}{\partial z} + \frac{\partial h_e}{\partial x} = 0, \quad h_e = \frac{\partial \eta}{\partial t}. \tag{61}$$

Equations (61) are complemented by the local Lamb-Helmholtz PDEs

$$\frac{\partial be_n}{\partial x} - \frac{\partial he_n}{\partial z} = 0, \quad \frac{\partial be_n}{\partial z} + \frac{\partial he_n}{\partial x} = 0, \quad he_n = \frac{\partial \eta_n}{\partial t}, \tag{62}$$

since the cumulative dynamic potentials are again decomposed into the local dynamic potentials

$$h_e = \sum_{n=1}^{N} he_n(x,z,t), \quad b_e = \sum_{n=1}^{N} be_n(x,z,t). \tag{63}$$

Construct a general term of the Bernoulli potential of the local flows in the KEF structure with time-dependent coefficients

$$be_n = \left[fb_n(t) ca_n + gb_n(t) sa_n \right] \exp(\mp \rho_n z). \tag{64}$$

Computation of the temporal derivative of η_n, application of (26) (27), substitution in (62), collection of the structural functions, and vanishing their coefficients reduce two Lamb-Helmholtz PDEs to the following system of four Lamb-Helmholtz AEs with respect to $fb_n(t)$ and $gb_n(t)$ for the upper flows

$$-\rho_n \left[fb_n(t) + Cx_n Gw_n(t) \right] + \frac{\mathrm{d}Fw_n}{\mathrm{d}t} = 0, \quad \rho_n \left[gb_n(t) - Cx_n Fw_n(t) \right] - \frac{\mathrm{d}Gw_n}{\mathrm{d}t} = 0, \tag{65}$$

$$-\rho_n \left[fb_n(t) + Cx_n Gw_n(t) \right] + \frac{\mathrm{d}Fw_n}{\mathrm{d}t} = 0, \quad -\rho_n \left[gb_n(t) - Cx_n Fw_n(t) \right] + \frac{\mathrm{d}Gw_n}{\mathrm{d}t} = 0, \tag{66}$$

and the lower flows

$$-\rho_n \left[fb_n(t) - Cx_n Gw_n(t) \right] - \frac{\mathrm{d}Fw_n}{\mathrm{d}t} = 0, \quad \rho_n \left[gb_n(t) + Cx_n Fw_n(t) \right] + \frac{\mathrm{d}Gw_n}{\mathrm{d}t} = 0, \tag{67}$$

$$\rho_n \left[fb_n(t) - Cx_n Gw_n(t) \right] + \frac{\mathrm{d}Fw_n}{\mathrm{d}t} = 0, \quad \rho_n \left[gb_n(t) + Cx_n Fw_n(t) \right] + \frac{\mathrm{d}Gw_n}{\mathrm{d}t} = 0, \tag{68}$$

and all variables, parameters, and functions $x, z, t, Xa_n, Cx_n, \rho_n, ca_n sa_n, fb_n(t), gb_n(t), Fw_n(t)$, and $Gw_n(t)$.

Solving AEs (65) and (67) for structural coefficients $fb_n(t)$ and $gb_n(t)$ yields for the upper and lower flows, respectively,

$$fb_n(t) = \mp \left[Cx_n Gw_n(t) - \frac{1}{\rho_n} \frac{\mathrm{d}Fw_n}{\mathrm{d}t} \right], \quad gb_n(t) = \pm \left[Cx_n Fw_n(t) + \frac{1}{\rho_n} \frac{\mathrm{d}Gw_n}{\mathrm{d}t} \right]. \tag{69}$$

Substitution of solutions (69) in AEs (66) and (68) reduces them to identities. Eventually, substitution of structural coefficients (69) in the KEF structure (64) and superpositions (63) returns the cumulative dynamic potentials in the KEF structures for the upper and lower cumulative flows, respectively,

$$he(x,z,t) = -\sum_{n=1}^{N} \left\{ \left[Cx_n Fw_n(t) + \frac{1}{\rho_n} \frac{\mathrm{d}Gw_n}{\mathrm{d}t} \right] ca_n + \left[Cx_n Gw_n(t) - \frac{1}{\rho_n} \frac{\mathrm{d}Fw_n}{\mathrm{d}t} \right] sa_n \right\} \exp(\mp \rho_n z), \tag{70}$$

$$be(x,z,t) = \pm \sum_{n=1}^{N} \left\{ -\left[Cx_n Gw_n(t) - \frac{1}{\rho_n} \frac{\mathrm{d}Fw_n}{\mathrm{d}t} \right] ca_n + \left[Cx_n Fw_n(t) + \frac{1}{\rho_n} \frac{\mathrm{d}Gw_n}{\mathrm{d}t} \right] sa_n \right\} \exp(\mp \rho_n z). \tag{71}$$

3.2. Theoretical Solutions for the Total Pressure in the KEF-DEF Structures

Theoretical dynamic problems in the KEF-DEF structures for k_e, p_d, and p_t of the cumulative flows are formulated by definition

$$k_e(x,z,t) = \frac{1}{2}\left[u(x,z,t)^2 + w(x,z,t)^2 \right], \tag{72}$$

the Bernoulli Equation (9) with $\phi = 0$

$$p_d(x,z,t) = b_e(x,z,t) - k_e(x,z,t), \tag{73}$$

and the hydrostatic Equation (5)

$$p_t(x,z,t) = p_0 - \rho g_z z + \rho p_d(x,z,t), \tag{74}$$

where p_0 is the reference pressure at $z = 0$.

Computation of k_e by (40) (41) and (34) returns

$$\begin{aligned} k_e(x,z,t) = &\frac{1}{2}\sum_{n=1}^{N}\left[Fw_n^2(t) + Gw_n^2(t)\right]\exp(\mp 2\rho_n z) + \sum_{n=1}^{N-1}\sum_{m=n+1}^{N}\left\{\left[Fw_n(t)Fw_m(t) + Gw_n(t)Gw_m(t)\right]Cad_{n,m}\right. \\ &\left. + \left[Fw_m(t)Gw_n(t) - Fw_n(t)Gw_m(t)\right]Sad_{n,m}\right\}\exp\left[\mp(\rho_n + \rho_m)z\right] \end{aligned} \tag{75}$$

for the upper and lower cumulative flows, respectively. Substitution of (71), (75), and (73) in (74) yields

$$\begin{aligned} p_t(x,z,t) = p_0 - \rho g_z z + \rho\Bigg(&\pm\sum_{n=1}^{N}\left\{-\left[Cx_n Gw_n(t) - \frac{1}{\rho_n}\frac{\mathrm{d}Fw_n}{\mathrm{d}t}\right]ca_n + \left[Cx_n Fw_n(t) + \frac{1}{\rho_n}\frac{\mathrm{d}Gw_n}{\mathrm{d}t}\right]sa_n\right\}\exp(\mp\rho_n z) \\ &-\frac{1}{2}\sum_{n=1}^{N}\left[Fw_n^2(t) + Gw_n^2(t)\right]\exp(\mp 2\rho_n z) - \sum_{n=1}^{N-1}\sum_{m=n+1}^{N}\left\{\left[Fw_n(t)Fw_m(t) + Gw_n(t)Gw_m(t)\right]Cad_{n,m}\right. \\ &\left. + \left[Fw_m(t)Gw_n(t) - Fw_n(t)Gw_m(t)\right]Sad_{n,m}\right\}\exp\left[\mp(\rho_n + \rho_m)z\right]\Bigg) \end{aligned} \tag{76}$$

for the upper and lower cumulative flows, respectively. So, the kinetic energy is obtained in the DEF structures, the dynamic pressure is expressed in the KEF-DEF structures, and the total pressure is computed in the KEF-DEF and polynomial structures.

3.3. Harmonic Relationships between the Kinematic and Dynamic Variables

Similar to the invariant trigonometric, hyperbolic, and elliptic structures [8], there are two pairs of independent KEF structures: generating structures with general terms As_n, Cs_n and complementary structures with general terms Bs_n, Ds_n for the upper and lower flows, respectively,

$$As_n = \left[Fw_n(t)ca_n + Gw_n(t)sa_n\right]\exp(\mp\rho_n z), \quad Bs_n = \left[Gw_n(t)ca_n - Fw_n(t)sa_n\right]\exp(\mp\rho_n z), \tag{77}$$

$$Cs_n = \left(\frac{\mathrm{d}Fw_n}{\mathrm{d}t}ca_n + \frac{\mathrm{d}Gw_n}{\mathrm{d}t}sa_n\right)\exp(\mp\rho_n z), \quad Ds_n = \left(\frac{\mathrm{d}Gw_n}{\mathrm{d}t}ca_n - \frac{\mathrm{d}Fw_n}{\mathrm{d}t}sa_n\right)\exp(\mp\rho_n z). \tag{78}$$

Expressing velocity components (34), kinematic potentials (60), and dynamic potentials (70) (71) through the generating and complementary structures (77) (78) and solving for As_n and Bs_n gives algebraic relationships

$$As_n = w_n = \mp\rho_n\varphi_n = -\frac{he_n}{Cx_n} - \frac{Ds_n}{\rho_n Cx_n}, \quad Bs_n = \mp u_n = -\rho_n\eta_n = \mp\frac{be_n}{Cx_n} + \frac{Cs_n}{\rho_n Cx_n}. \tag{79}$$

Taking derivatives of (34) and (60) with respect to *x*, *z* and solving for As_n and Bs_n yields differential relationships, which extend algebraic ones (79),

$$As_n = \pm\frac{1}{\rho_n}\frac{\partial u_n}{\partial x} = \mp\frac{1}{\rho_n}\frac{\partial w_n}{\partial z} = \frac{\partial \eta_n}{\partial x} = \frac{\partial \varphi_n}{\partial z}, \quad Bs_n = \frac{1}{\rho_n}\frac{\partial w_n}{\partial x} = \frac{1}{\rho_n}\frac{\partial u_n}{\partial z} = \mp\frac{\partial \varphi_n}{\partial x} = \pm\frac{\partial \eta_n}{\partial z}. \tag{80}$$

In fluid dynamics, relationships (79) (80) mean that a harmonic flow, which is non-uniform in x- or z-directions, produces a complementary flow in *z*- or *x*-directions, respectively.

Computing velocity components (34) and dynamic potentials (70) (71) through the generating and complementary structures (77) (78), taking temporal and spatial derivatives, and solving for be_n and he_n returns

$$\rho_n he_n = \pm\frac{\partial u_n}{\partial t} = \mp\frac{\partial be_n}{\partial x} = \mp\frac{\partial he_n}{\partial z}, \quad \rho_n be_n = \pm\frac{\partial w_n}{\partial t} = \pm\frac{\partial he_n}{\partial x} = \mp\frac{\partial be_n}{\partial z}. \tag{81}$$

Differential relationships (81) mean that spatial derivatives of the dynamic potentials generate temporal rates of a harmonic flow.

By the following substitutions:

$$u_n = u = \eta_n = \eta = he_n = he = u_c, \quad -w_n = -w = \phi_n = \phi = -be_n = -be = v_c, \tag{82}$$

both local and global vorticity and continuity Equations (12) and (14), Helmholtz Equations (48)-(49) and (51)-(52), and Lamb-Helmholtz Equations (61) and (62), respectively, are reduced to the Cauchy-Riemann equations

$$\frac{\partial u_c}{\partial x} - \frac{\partial v_c}{\partial z} = 0, \quad \frac{\partial u_c}{\partial z} + \frac{\partial v_c}{\partial x} = 0 \tag{83}$$

for conjugate functions u_c and v_c [4]. All conjugate functions have orthogonal isocurves, due to the vanishing scalar product of gradients,

$$\nabla u_c \cdot \nabla v_c = \frac{\partial u_c}{\partial x}\frac{\partial v_c}{\partial x} + \frac{\partial u_c}{\partial z}\frac{\partial v_c}{\partial z} = 0, \tag{84}$$

and vanishing Laplacians,

$$\frac{\partial^2 u_c}{\partial x^2} + \frac{\partial^2 u_c}{\partial z^2} = 0, \quad \frac{\partial^2 v_c}{\partial x^2} + \frac{\partial^2 v_c}{\partial z^2} = 0. \tag{85}$$

Thus, $(u_n, w_n), (u, w), (\eta_n, \phi_n), (\eta, \phi), (he_n, be_n)$, and (he, be) are six pairs of harmonic functions with orthogonal isocurves.

3.4. Theoretical Verification by the System of Navier-Stokes PDEs

The system of the Navier-Stokes PDEs (1)-(2) in the scalar notation becomes

$$\frac{\partial u}{\partial t} + u\frac{\partial u}{\partial x} + w\frac{\partial u}{\partial z} = -\frac{1}{\rho}\frac{\partial p_t}{\partial x} + \nu\left(\frac{\partial^2 u}{\partial x^2} + \frac{\partial^2 u}{\partial z^2}\right), \quad \frac{\partial w}{\partial t} + u\frac{\partial w}{\partial x} + w\frac{\partial w}{\partial z} = -\frac{1}{\rho}\frac{\partial p_t}{\partial z} + \nu\left(\frac{\partial^2 w}{\partial x^2} + \frac{\partial^2 w}{\partial z^2}\right) - g_z, \tag{86}$$

$$\frac{\partial u}{\partial x} + \frac{\partial w}{\partial z} = 0. \tag{87}$$

Computation of spatial derivatives of (34) by (26)-(27) reduces (87) to identity both for the upper and lower cumulative flows.

Temporal derivatives of $\boldsymbol{v}$ in the KEF structures for the upper and lower cumulative flows, respectively, are

$$\frac{\partial u}{\partial t} = \mp\sum_{n=1}^{N}\left\{\left[\rho_n Cx_n Fw_n(t) + \frac{\mathrm{d}Gw_n}{\mathrm{d}t}\right]ca_n + \left[\rho_n Cx_n Gw_n(t) - \frac{\mathrm{d}Fw_n}{\mathrm{d}t}\right]sa_n\right\}\exp(\mp\rho_n z), \tag{88}$$

$$\frac{\partial w}{\partial t} = \sum_{n=1}^{N}\left\{-\left[\rho_n Cx_n Gw_n(t) - \frac{\mathrm{d}Fw_n}{\mathrm{d}t}\right]ca_n + \left[\rho_n Cx_n Fw_n(t) + \frac{\mathrm{d}Gw_n}{\mathrm{d}t}\right]sa_n\right\}\exp(\mp\rho_n z). \tag{89}$$

The directional derivatives of (86) computed by (40)-(41) in the DEF structures for the upper and lower cumulative flows, respectively, become

$$\begin{aligned}(\boldsymbol{v}\cdot\nabla)u = \sum_{n=1}^{N-1}\sum_{m=n+1}^{N}&\{[Fw_n(t)Gw_m(t) - Fw_m(t)Gw_n(t)]Cad_{n,m}\\ &+[Fw_n(t)Fw_m(t) + Gw_n(t)Gw_m(t)]Sad_{n,m}\}(\rho_m - \rho_n)\exp[\mp(\rho_n + \rho_m)z],\end{aligned} \tag{90}$$

$$\begin{aligned}(\boldsymbol{v}\cdot\nabla)w = \mp\sum_{n=1}^{N}\left[Fw_n^2(t) + Gw_n^2(t)\right]\exp(\mp 2\rho_n z) \mp \sum_{n=1}^{N-1}\sum_{m=n+1}^{N}&\{[Fw_n(t)Fw_m(t) + Gw_n(t)Gw_m(t)]Cad_{n,m}\\ -[Fw_n(t)Gw_m(t) - Fw_m(t)Gw_n(t)]Sad_{n,m}\}&(\rho_m + \rho_n)\exp[\mp(\rho_n + \rho_m)z].\end{aligned} \tag{91}$$

By using (26)-(27), components of the gradient of (76) may be written in the KEF-DEF structures for the upper and lower cumulative flows, respectively, as

$$\frac{\partial p_t}{\partial x}=\rho\left(\pm\sum_{n=1}^{N}\left\{\left[\rho_n Cx_n Fw_n(t)+\frac{\mathrm{d}Gw_n}{\mathrm{d}t}\right]ca_n+\left[\rho_n Cx_n Gw_n(t)-\frac{\mathrm{d}Fw_n}{\mathrm{d}t}\right]sa_n\right\}\exp(\mp\rho_n z)\right.$$
$$-\sum_{n=1}^{N-1}\sum_{m=n+1}^{N}\left\{\left[Fw_n(t)Gw_m(t)-Fw_m(t)Gw_n(t)\right]Cad_{n,m}\right. \tag{92}$$
$$\left.\left.+\left[Fw_n(t)Fw_m(t)+Gw_n(t)Gw_m(t)\right]Sad_{n,m}\right\}(\rho_m-\rho_n)\exp\left[\mp(\rho_n+\rho_m)z\right]\right),$$

$$\frac{\partial p_t}{\partial z}=\rho\left(-g_z+\sum_{n=1}^{N}\left\{\left[\rho_n Cx_n Gw_n(t)-\frac{\mathrm{d}Fw_n}{\mathrm{d}t}\right]ca_n-\left[\rho_n Cx_n Fw_n(t)+\frac{\mathrm{d}Gw_n}{\mathrm{d}t}\right]sa_n\right\}\exp(\mp\rho_n z)\right.$$
$$\pm\sum_{n=1}^{N}\left[Fw_n^2(t)+Gw_n^2(t)\right]\rho_n\exp(\mp2\rho_n z)\pm\sum_{n=1}^{N-1}\sum_{m=n+1}^{N}\left\{\left[Fw_n(t)Fw_m(t)+Gw_n(t)Gw_m(t)\right]Cad_{n,m}\right. \tag{93}$$
$$\left.\left.-\left[Fw_n(t)Gw_m(t)-Fw_m(t)Gw_n(t)\right]Sad_{n,m}\right\}(\rho_m+\rho_n)\exp\left[\mp(\rho_n+\rho_m)z\right]\right).$$

Substitution of Equations (88)-(93) and (85) for u and w in (86) reduces then to identities. Thus, Equations (34) and (76) constitute exact solutions in the KEF, DEF, and KEF-DEF structures with time-dependent structural coefficients for deterministic chaos of N stochastic waves both in the upper and lower domains.

The theoretical solutions in the KEF, DEF, and KEF-DEF structures for the dynamic problems of Section 3 were computed by theoretical programming methods with symbolic general terms in the virtual environment of the global variable *Eqt* with 14 procedures of 410 code lines in total. The theoretical solutions for Helmholtz and Bernoulli potentials (70)-(71), total pressure (76), temporal derivatives (88)-(89), directional derivatives (90)-(91), and pressure gradient (92)-(93) of the upper and lower cumulative flows were justified by the correspondent experimental solutions for N = 1, 3, 10.

All kinematic solutions of Section 2 and dynamic solutions of Section 3 with time-dependent structural coefficients are reduced to the correspondent solutions of [5] when $Fw_n(t)=Fw_n$ and $Gw_n(t)=Gw_n$.

4. Chaotic Scenarios

Boundary functions $Fw_n(t)$ and $Gw_n(t)$, which are shown in **Figure 2** for $n=3$, are constructed from stochastic solutions of the Navier-Stokes equation in one dimension by the following method. Let $Fd_n(x_d,\tau)$ and $Gd_n(x_d,\tau)$ be the stochastic solutions of

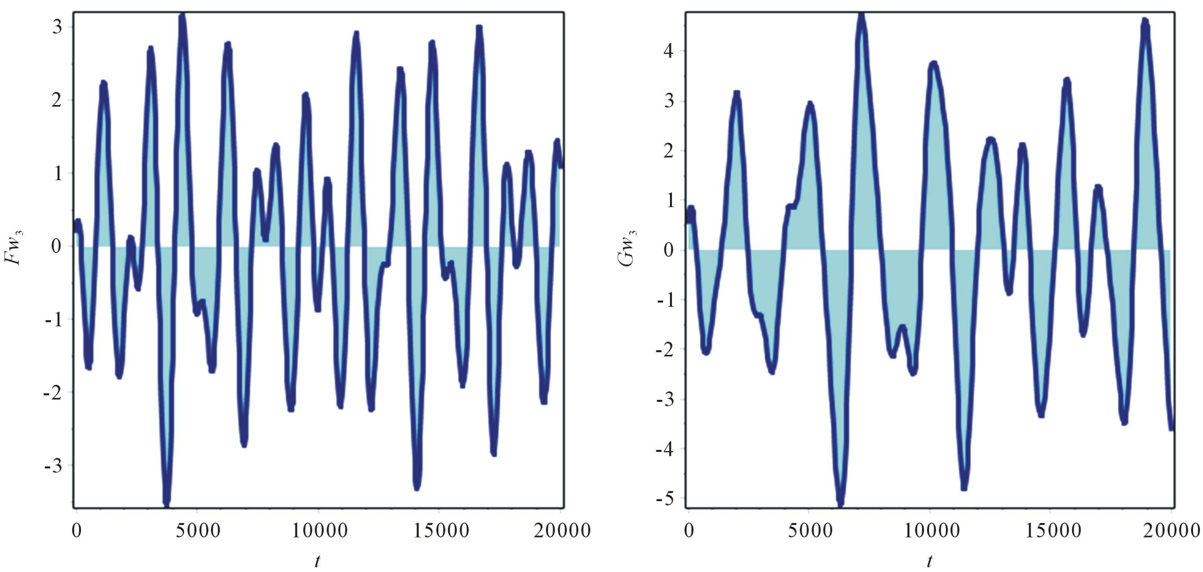

Figure 2. Stochastic boundary functions.

$$R_n \frac{\partial Fd_n}{\partial \tau} - \frac{\partial^2 Fd_n}{\partial x_d^2} = 0, \quad R_n \frac{\partial Gd_n}{\partial \tau} - \frac{\partial^2 Gd_n}{\partial x_d^2} = 0, \tag{94}$$

where R_n is the Reynolds number.

In agreement with [7], $Fd_n(x_d, \tau)$ is composed of an invariant structure with even indices of hyperbolic secant-tangent temporal modes and trigonometric sine spatial modes (HETO structure) and an invariant structure of the same temporal modes combined with trigonometric cosine spatial modes (HETE structure)

$$\begin{aligned} Fd_n &= \sum_{m=1}^{n} \left(th_{n,m} \sum_{k=1}^{K} gd_{n,2k,m} sh_{n,2k,m} + \sum_{k=1}^{K} fd_{n,2k,m} sh_{n,2k,m} \right), \\ gd_{n,2k,m} &= \sum_{l=1}^{k} a_{2k,2l} \left(A_{n,2l,m} sn_{n,2l,m} + B_{n,2l,m} cs_{n,2l,m} \right), \\ fd_{n,2k,m} &= \sum_{l=1}^{k} b_{2k,2l} \left(A_{n,2l,m} sn_{n,2l,m} + B_{n,2l,m} cs_{n,2l,m} \right). \end{aligned} \tag{95}$$

$Gd_n(x_d, \tau)$ is formed of an invariant structure with odd indices of hyperbolic secant-tangent temporal modes and trigonometric sine spatial modes (HOTO structure) and an invariant structure of the same temporal modes composed with trigonometric cosine spatial modes (HOTE structure)

$$\begin{aligned} Gd_n &= \sum_{m=1}^{n} \left(th_{n,m} \sum_{k=1}^{K} gd_{n,2k-1,m} sh_{n,2k-1,m} + \sum_{k=1}^{K} fd_{n,2k-1,m} sh_{n,2k-1,m} \right), \\ gd_{n,2k-1,m} &= \sum_{k=1}^{K} a_{2k-1,2l-1} \left(A_{n,2l-1,m} sn_{n,2l-1,m} + B_{n,2l-1,m} cs_{n,2l-1,m} \right), \\ fd_{n,2k-1,m} &= \sum_{l=1}^{k} b_{2k-1,2l-1} \left(A_{n,2l-1,m} sn_{n,2l-1,m} + B_{n,2l-1,m} cs_{n,2l-1,m} \right). \end{aligned} \tag{96}$$

Here, a structural notation

$$\begin{aligned} & th_{n,m} = \tanh\left(\delta_{n,m}\right), \ sh_{n,2k,m} = \operatorname{sech}^{2k}\left(\delta_{n,m}\right), \ sh_{n,2k-1,m} = \operatorname{sech}^{2k-1}\left(\delta_{n,m}\right), \ \delta_{n,m} = \omega_{n,m}\left(\tau - \tau_{n,m}\right), \\ & sn_{n,2l,m} = \sin\left(\kappa_{n,2l,m} x_d\right), \ cs_{n,2l,m} = \cos\left(\kappa_{n,2l,m} x_d\right), \ sn_{n,2l-1,m} = \sin\left(\kappa_{n,2l,m} x_d\right), \\ & cs_{n,2l-1,m} = \cos\left(\kappa_{n,2l,m} x_d\right), \ \kappa_{n,2l,m} = \sqrt{R_n \omega_{n,m} 2l}, \ \kappa_{n,2l-1,m} = \sqrt{R_n \omega_{n,m}(2l-1)} \end{aligned} \tag{97}$$

is used for structural functions of temporal and spatial modes, where $m = 1, 2, \cdots, n$ is an index of spatiotemporal components, $k = 1, 2, \cdots, K$ is an index of temporal modes, $l = 1, 2, \cdots, k$ is an index of spatial modes, $\omega_{n,m}$ is a frequency, $\tau_{n,m}$ is a delay parameter, $A_{n,2l,m}$, $B_{n,2l,m}$, $A_{n,2l-1,m}$, and $B_{n,2l-1,m}$ are spatial amplitudes. Structural coefficients $a_{2k,2l}$, $b_{2k,2l}$, $a_{2k-1,2l-1}$, and $b_{2k-1,2l-1}$ are computed by initialization conditions

$$a_{2k,2l} = 1, \ b_{2k,2l} = 1, \ a_{2k-1,2l-1} = 1, \ b_{2k-1,2l-1} = 1, \tag{98}$$

and recurrent relations

$$\begin{aligned} b_{2k,2l} &= \frac{(2k-1)(k-1)}{2(k-l)(k+l)} b_{2k-2,2l}, \quad b_{2k-1,2l-1} = \frac{(2k-3)(k-1)}{2(k-l)(k+l-1)} b_{2k-3,2l-1}, \\ a_{2k,2l} &= \frac{k}{l} b_{2k,2l}, \quad a_{2k-1,2l-1} = \frac{2k-1}{2l-1} b_{2k-1,2l-1}. \end{aligned} \tag{99}$$

In **Figure 2**, stochastic boundary functions

$$Fw_n(t) = Fd_n(t, Xa_n T_0), \quad Gw_n(t) = Gd_n(t, Xa_n T_0) \tag{100}$$

were evaluated for $N = 3$, $K = 5$, $R_n = 10n^2$, temporal delays $\tau_{n,m} = T_0 m$, a scale of temporal delays $T_0 = 10^6$, $Xa_n = (3/2, 1, 1/2)$, scales of spatiotemporal components

$$C_h = 1, \quad C_l = -12/5, \quad C_m = C_h + C_l\left[1 + (-1)^m\right]/2 \tag{101}$$

and spatial amplitudes

$$A_{n,2l,m} = B_{n,2l,m} = C_m/(2l)!, \quad A_{n,2l-1,m} = B_{n,2l-1,m} = C_m/(2l-1)!, \tag{102}$$

which insure convergence of the spatial modes. Frequencies of $Fd_n(x_d,\tau)$:

$$\omega_{1,1} = 1.847\times10^{-6},\ \omega_{2,1} = 4.617\times10^{-7},\ \omega_{2,2} = 1.649\times10^{-7},$$
$$\omega_{3,1} = 2.052\times10^{-7},\ \omega_{3,2} = 7.329\times10^{-8},\ \omega_{3,3} = 1.026\times10^{-7},$$

and frequencies of $Gd_n(x_d,\tau)$:

$$\omega_{1,1} = 1.370\times10^{-6},\ \omega_{2,1} = 3.424\times10^{-7},\ \omega_{2,2} = 1.223\times10^{-7},$$
$$\omega_{3,1} = 1.522\times10^{-7},\ \omega_{3,2} = 5.435\times10^{-8},\ \omega_{3,3} = 7.609\times10^{-7},$$

were computed by iterations from tolerance equations

$$\begin{gathered} R_n(2K+1)\sum_{m=1}^{n}\omega_{n,m}\sum_{l=1}^{K}a_{2K,2l}\left(\left|A_{n,2l,m}\right|+\left|B_{n,2l,m}\right|\right) = 2d_c, \\ R_n 2K\sum_{m=1}^{n}\omega_{n,m}\sum_{l=1}^{K}a_{2K-1,2l-1}\left(\left|A_{n,2l-1,m}\right|+\left|B_{n,2l-1,m}\right|\right) = 2d_c. \end{gathered} \tag{103}$$

These equations guarantee that absolute values of remainders of the structural approximations of (94)

$$rm_{n,2K}(x_d,\tau) = -R_n(2K+1)\sum_{m=1}^{n}\omega_{n,m}sh_{n,2K+2,m}\sum_{l=1}^{K}a_{2K,2l}\left(A_{n,2l,m}sn_{n,2l,m}+B_{n,2l,m}cs_{n,2l,m}\right), \tag{104}$$

$$rm_{n,2K-1}(x_d,\tau) = R_n(2K)\sum_{m=1}^{n}\omega_{n,m}sh_{n,2K+1,m}\sum_{l=1}^{K}a_{2K-1,2l-1}\left(A_{n,2l-1,m}sn_{n,2l-1,m}+B_{n,2l-1,m}cs_{n,2l-1,m}\right) \tag{105}$$

do not exceed $2d_c$ for all n, x_d, and τ, where $d_c = 10^{-4}$ is an admissible error of computation of an invariant structure. Chaotic behavior of the boundary functions increases with *n*, *K*, and, especially, R_n, while various chaotic scenarios are modeled by $N\left[(N+1)(2K+1)+2\right]$ parameters R_n, Xa_n, $\omega_{n,m}$, $\tau_{n,m}$, $A_{n,2l,m}$, $B_{n,2l,m}$, $A_{n,2l-1,m}$, and $B_{n,2l-1,m}$.

The KEF structures and KEF-DEF structures are visualized in **Figure 3** by instantaneous 3d surface plots with isocurves at $t = 1.2\times10^6$ for scalar potential ϕ (60) and the dynamic pressure $p_d = g_z z + \left[p_t(x,z,t) - p_0\right]/\rho$ with p_t from (76), respectively. Local minimums of the KEF-DEF structure for p_d coincides with local maximums of the DEF structure for k_e, in agreement with [1]. The spatial structure of ϕ and p_d for stochastic waves coincides with that shown in **Figure 2** and **Figure 3** of [5] for conservative

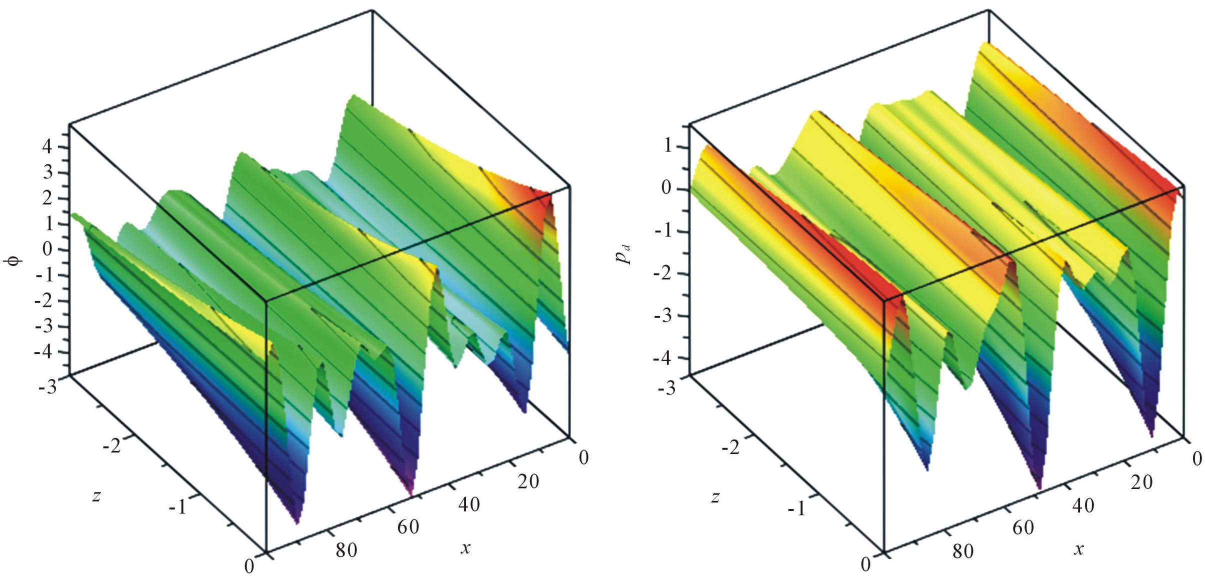

Figure 3. Scalar potential (left) and dynamic pressure (right) of the lower cumulative flow.

waves. The temporal structure of ϕ and p_d for stochastic waves, which is visualized by animations, significantly differs from that of ϕ and p_d for conservative waves because of the chaotic behavior of boundary functions $Fw_n(t)$ and $Gw_n(t)$.

5. Conclusions

The computational method of solving PDEs by decomposition in invariant structures, which continues the analytical methods of separation of variables and undetermined coefficients, is generalized in the current paper at the KEF, DEF, and KEF-DEF structures with time-dependent coefficients. This computational method is implemented in the kinematic and dynamic problems for internal waves by 43 procedures with 1070 code lines of the experimental computing in total and 35 procedures with 932 code lines of the theoretical computing in total. These structures with time-dependent structural coefficients are invariant with respect to various differential and algebraic operations.

For internal waves vanishing at infinity in the upper and lower domains, the Dirichlet problems are formulated for the kinematic and dynamic systems of the vorticity, continuity, Helmholtz, Lamb-Helmholtz, and Bernoulli equations. The exact solutions of the Navier-Stokes PDEs for the deterministic chaos of N stochastic waves are revealed experimentally, proved theoretically, and justified by the system of Navier-Stokes PDEs in the class of flows with the harmonic velocity field. The kinematic and dynamic solutions for stochastic waves coincide with the correspondent solutions for conservative waves [5] when stochastic boundary functions are reduced to constants.

Independence of both propagating and interacting internal waves is shown by computation of the Jacobian determinants in the DEF structures. Conditions for existence of parallel and orthogonal waves with time-dependent amplitudes are obtained through the Jacobian determinants, as well. The harmonic relationships between six pairs of the harmonic, fluid-dynamic variables, their temporal derivatives, and their spatial derivatives with respect to x and z are derived both for the upper and lower flows.

The stochastic boundary functions are constructed from the stochastic solutions of the one-dimensional Navier-Stokes equation [7] with hyperbolic temporal modes and trigonometric spatial modes in the HETO, HETE, HOTO, and HOTE structures. Various scenarios of a developed wave chaos are modeled by $3N$ parameters for internal waves and $2N$ stochastic boundary functions, which depend on $N\left[(N+1)(2K+1)+2\right]$ parameters, where K is a number of temporal modes.

Acknowledgements

The author thanks S. P. Bhavaraju for the stimulating discussion at the 2013 SIAM Annual Meeting. Support of the College of Mount Saint Vincent and CAAM is gratefully acknowledged.

References

[1] Lamb, S.H. (1945) Hydrodynamics. 6th Edition, Dover Publications, New York.

[2] Pozrikidis, C. (2011) Introduction to Theoretical and Computational Fluid Dynamics. 2nd Edition, Oxford University Press, Oxford.

[3] Miroshnikov, V.A. (2005) The Boussinesq-Rayleigh Series for Two-Dimensional Flows away from Boundaries. *Applied Mathematics Research Express*, **2005**, 183-227. http://dx.doi.org/10.1155/AMRX.2005.183

[4] Korn, G.A. and Korn, T.A. (2000) Mathematical Handbook for Scientists and Engineers: Definitions, Theorems, and Formulas for Reference and Review. 2nd Revised Edition, Dover Publications, New York.

[5] Miroshnikov, V.A. (2014) Nonlinear Interaction of *N* Conservative Waves in Two Dimensions. *American Journal of Computational Mathematics*, **4**, 127-142. http://dx.doi.org/10.4236/ajcm.2014.43012

[6] Kochin, N.E., Kibel, I.A. and Roze, N.V. (1964) Theoretical Hydromechanics. John Wiley & Sons Ltd., Chichester.

[7] Miroshnikov, V.A. (2009) Spatiotemporal Cascades of Exposed and Hidden Perturbations of the Couette Flow. *Advances and Applications in Fluid Dynamics*, **6**, 141-165.

[8] Miroshnikov, V.A. (2012) Dual Perturbations of the Poiseuille-Hagen Flow in Invariant Elliptic Structures. *Advances and Applications in Fluid Dynamics*, **11**, 1-58.